

Surface Structure of Solutions of Polyvinyl Alcohol in Water

Carolyn J Moll, Konrad Meister, Johannes Kirschner, and Huib J. Bakker

J. Phys. Chem. B, **Just Accepted Manuscript** • DOI: 10.1021/acs.jpcc.8b08374 • Publication Date (Web): 29 Oct 2018

Downloaded from <http://pubs.acs.org> on November 8, 2018

Just Accepted

“Just Accepted” manuscripts have been peer-reviewed and accepted for publication. They are posted online prior to technical editing, formatting for publication and author proofing. The American Chemical Society provides “Just Accepted” as a service to the research community to expedite the dissemination of scientific material as soon as possible after acceptance. “Just Accepted” manuscripts appear in full in PDF format accompanied by an HTML abstract. “Just Accepted” manuscripts have been fully peer reviewed, but should not be considered the official version of record. They are citable by the Digital Object Identifier (DOI®). “Just Accepted” is an optional service offered to authors. Therefore, the “Just Accepted” Web site may not include all articles that will be published in the journal. After a manuscript is technically edited and formatted, it will be removed from the “Just Accepted” Web site and published as an ASAP article. Note that technical editing may introduce minor changes to the manuscript text and/or graphics which could affect content, and all legal disclaimers and ethical guidelines that apply to the journal pertain. ACS cannot be held responsible for errors or consequences arising from the use of information contained in these “Just Accepted” manuscripts.



1
2
3
4 **Surface Structure of Solutions of Polyvinyl Alcohol in Water**
5

6
7 **Authors:** C. J. Moll¹, K. Meister^{1,2*}, J. Kirschner & H. J. Bakker¹
8

9
10 **Affiliations:**
11

12 ¹AMOLF, Science Park 104, 1098XG Amsterdam, The Netherlands
13

14 ²Max-Planck Institute for Polymer Research, Ackermanweg 10, D-55128Mainz, Germany
15

16
17 *Correspondence to: K.Meister@amolf.nl
18
19
20

21 **Classification:**
22

23 Physical Sciences, Chemistry
24
25
26
27
28
29
30
31
32
33
34
35
36
37
38
39
40
41
42
43
44
45
46
47
48
49
50
51
52
53
54
55
56
57
58
59
60

Abstract:

We use surface-specific heterodyne-detected vibrational sum-frequency generation spectroscopy (HD-VSFG) and surface tension measurements to investigate the molecular structure of the surface of aqueous solutions of polyvinyl alcohol (PVA) polymers with average molecular weights of 10000 g/mol and 125000 g/mol. We find that the interfacial water molecules have a preferred orientation with their hydrogen-bonded O-H groups pointing away from the bulk, for both PVA₁₀₀₀₀ and PVA₁₂₅₀₀₀. This observation is explained from the ongoing hydrolysis of the acetyl impurities on the PVA polymer chains. This hydrolysis yields negatively charged acetate ions that have a relatively high surface propensity. For both PVA₁₀₀₀₀ and PVA₁₂₅₀₀₀ the strong positive signal vanishes when the pH is decreased, due to the neutralization of the acetate ions. For solutions with a high concentration of PVA₁₀₀₀₀ the interfacial water signal becomes very small, indicating that the surface gets completely covered with a disordered PVA polymer film. In contrast, for high concentrations of PVA₁₂₅₀₀₀ the strong positive water signal persists at high pH, which shows that the water surface does not get completely covered. The HD-VSFG data combined with surface tension data indicate that concentrated PVA₁₂₅₀₀₀ solutions form a structured surface layer with pores containing a high density of interfacial water.

Introduction:

In the last decades synthetic polymers have gained tremendous attention since they can be fabricated in various shapes and structures and with a wide range of physical and chemical properties. Current research on synthetic polymers is strongly focused on the production of nontoxic, biodegradable polymers and their applications in biomedicine and material technologies^{1,2,3}. Polyvinyl alcohol (PVA) is a well-known synthetic polymer that has a large number of desirable properties like water affinity, non-toxicity, biocompatibility, biodegradability and the flexibility to form networks⁴. It is widely used in applications ranging from membrane-based liquid and gas mixture separation to material technologies and encapsulation of bacteria via electrospinning^{5,6,7}. PVA-based systems are further used for controlled drug delivery, medical imaging enhancement and cell interactions where the characteristics of the interface between PVA and the external medium plays an important role in determining the physicochemical stability and affinity toward biological systems⁸. PVA has further been reported to have remarkable properties at the ice-water interface⁹. It is a very potent compound to inhibit ice recrystallization and was proposed to be able to bind to ice, a property that was long believed to be unique for antifreeze proteins^{10,11}.

The behaviour of PVA at interfaces is currently poorly understood despite its high relevance for numerous technologies⁴. The reason for this lack of knowledge is the limited number of molecular probing techniques that are capable of selectively measuring the interface in aqueous solution. Up to now, surface tension measurements have been the main tool to investigate PVA at the water-air interface^{12,13}.

PVA has an amphiphilic nature with alternating hydrophobic methylene and hydrophilic hydroxyl groups as shown in the inset in Figure 1. In the diluted regime PVA behaves like a surfactant and decreases the surface tension γ of water with increasing polymer concentration¹². The degree of the decrease in surface tension can be influenced by the molecular weight, the stereochemistry, and the presence of charge impurities on the PVA polymer^{13,14,15}. At concentrations higher than ~4% the surface tension of PVA₁₂₅₀₀₀ solutions behaves anomalously and starts to increase with increasing PVA concentration⁴. For concentrations >10% the surface tension of the PVA solution is similar to that of pure water⁴. This anomaly was first noticed in the 1980s and has been observed in several studies of concentrated PVA solutions^{13, 16}.

1
2
3 Here we use heterodyne-detected vibrational sum-frequency generation spectroscopy (HD-VSFG)
4 to investigate the structure and conformation of PVA at the water-air interface, and to unravel the
5 molecular origin of the anomalous surface tension behaviour of PVA. VSFG is a highly surface-
6 specific technique that is ideally suited for the study of molecules adsorbed at interfaces¹⁷. In
7 VSFG an infrared light pulse and a visible pulse are combined to generate light at their sum-
8 frequency. The generation is enhanced in case the infrared light is resonant with a molecular
9 vibration. For the bulk, the generation of sum-frequency is symmetry forbidden. VSFG techniques
10 have been successfully used to investigate polymers at interfaces and were demonstrated to provide
11 molecular details on the conformation and solvent interactions of the molecule of interest^{18,19,20}.
12 By interfering the VSFG signal from the sample with a reference sum-frequency field, we
13 determine the phase of the generated sum-frequency light and thereby the phase of the second-
14 order optical susceptibility $\chi^{(2)}$. The real (Re) and imaginary (Im) parts of $\chi^{(2)}$ provide direct
15 information on the orientation of the vibrational transition dipole moments at the surface. This
16 heterodyne-detected VSFG thus provides unique information on the absolute molecular
17 orientation²¹.
18
19
20
21
22
23
24
25
26
27
28
29

30 **Material & Methods:**

31
32 The laser source for the vibrational sum-frequency generation experiments is a regenerative
33 Ti:Sapphire amplifier (Coherent) producing 800 nm pulses at a 1 kHz repetition rate with a pulse
34 duration of ~ 35 fs and a pulse energy of ~ 3.5 mJ. Approximately one third of the laser output is
35 used to pump a home-built optical parametric amplifier and a difference-frequency mixing stage.
36 This nonlinear frequency conversion produces broadband mid-IR pulses (tuneable from 2-10 μm ,
37 with a bandwidth of 600 cm^{-1} (FWHM), and a pulse energy of 10-20 μJ). In the current study the
38 mid-IR pulse was centred at $\sim 3\text{ }\mu\text{m}$ and had pulse energies of $\sim 15\text{ }\mu\text{J}$. Another part of the 800 nm
39 pulse is sent through an etalon to narrow down its bandwidth to $\sim 15\text{ cm}^{-1}$. The resulting narrow-
40 band 800 nm pulse (VIS) and the broadband IR pulse are directed to the sample surface at angles
41 of $\sim 50^\circ$ and $\sim 55^\circ$, respectively, to generate light at the sum frequency. The VIS and IR beams are
42 focused in spatial and temporal overlap on the sample surface with 200 mm and 100 mm focal
43 length lenses, respectively. The visible focus is located ~ 0.5 cm above the sample surfaces.
44
45
46
47
48
49
50
51
52
53

54 The SFG light generated at the surface is passed to a monochromator and detected with an
55 Electron-Multiplied Charge Coupled Device (EMCCD, Andor Technologies). Heterodyne-
56
57

1
2
3 detected VSGF is used to determine the imaginary and real parts of $\chi^{(2)}$. In HD-VSGF the SFG
4 electric field generated from the sample is combined with that of a local oscillator (LO, gold) at
5 the same frequency. The LO sum-frequency (LO-SFG) light is generated by first focusing the IR
6 and VIS beams on a metal surface to generate a strong non-resonant $\chi^{(2)}$ SFG signal. This signal is
7 delayed with respect to the IR and VIS beams by passing it through a silica plate (~ 1 mm). The
8 LO-SFG and the IR and VIS beams are refocused on the sample surface using a spherical mirror.
9 The IR and VIS beam generate the SFG signal of the sample. Subsequently, the LO-SFG and
10 sample SFG beams are collimated, sent into a monochromator and detected with a CCD.
11
12

13
14
15
16
17
18 The detected interference pattern contains cross terms from which we extract the real and
19 imaginary $\chi^{(2)}$ part using Fourier transformation. To obtain the $\text{Im } \chi^{(2)}$ of the sample, we compare
20 the signal with the HD-VSGF signal of a reference sample for which the phase of the SFG light is
21 known. For this purpose we use a z-cut quartz crystal. For HD-VSGF measurements it is crucial
22 that the HD-VSGF signal from the reference (z-cut quartz crystal) is generated at the same height
23 as the sample. A mismatch in height would result in a phase shift of the recorded spectra and thus
24 in the extracted real and imaginary $\chi^{(2)}$. We control the height of the reference quartz crystal and
25 the sample by monitoring the position of the VSGF signal on the CCD camera. This enables us to
26 define the SFG signal on the camera with a precision of 1 pixel size ($16 \times 16 \mu\text{m}$). In combination
27 with our setup geometry this results in a phase uncertainty of $\sim \pi/10$ (~ 20 degrees). The typical
28 acquisition time of a HD-VSGF spectrum is 120 s.
29
30
31
32
33
34
35
36

37
38 All VSGF measurements were performed in H_2O (Millipore). The polyvinyl alcohol samples are
39 specified in weight %. The pH value (Mettler Toledo FE20) of the samples was adjusted using
40 hydrochloric acid or sodium hydroxide. The pH was checked before and after each measurement.
41 The surface tension measurements (Kibron, DeltaPi) were performed at room temperature using
42 the Wilhelmy plate method. The measurements were performed using a multiwall plate, and were
43 repeated at least three times. Polyvinyl alcohol samples were acquired from Sigma Aldrich and
44 were used without further purification. The PVA samples differ in their molecular weight and
45 degree of hydrolysis. PVA is unlike most vinyl polymers not prepared by the polymerization of
46 the corresponding monomer since the monomer, vinyl alcohol, is unstable with respect to
47 acetaldehyde²². PVA is prepared by first polymerizing vinyl acetate, and the resulting polyvinyl
48 acetate is converted to PVA via hydrolysis. This process is often incomplete and a number of
49
50
51
52
53
54
55
56
57
58
59
60

1
2
3 charge impurities (acetyl groups) remain. The average molecular weight of the smaller PVA
4 (PVA₁₀₀₀₀) polymer was 10,000 g/mol with a hydrolysis degree of ~80%, which means that ~20%
5 of the acetyl groups have not been hydrolyzed to hydroxyl groups. The larger PVA (PVA₁₂₅₀₀₀)
6 polymer has an average molecular weight of 125,000 g/mol and a hydrolysis degree of ~98%.
7 Solutions were prepared by dissolving PVA in ultrapure water (Millipore) at high temperature (80-
8 90 °C). Due to the presence of the acetyl groups, the PVA can undergo spontaneous hydrolysis of
9 the ester groups of the PVA molecules, a process that is enhanced in acidic or basic aqueous media
10 and that is schematically shown in the Supporting Figures 1 and 2. The hydrolysis leads to the
11 release of acetic acid in neutral or acidic solution, or acetate in basic solution. The acetic acid
12 molecules will partly deprotonate, thus decreasing the pH and creating negative acetate ions (Fig.
13 S3). The negative acetate ions have a strong affinity for the water surface²³.
14
15
16
17
18
19
20
21
22
23
24
25
26
27
28
29
30
31
32
33
34
35
36
37
38
39
40
41
42
43
44
45
46
47
48
49
50
51
52
53
54
55
56
57
58
59
60

Results and Discussion

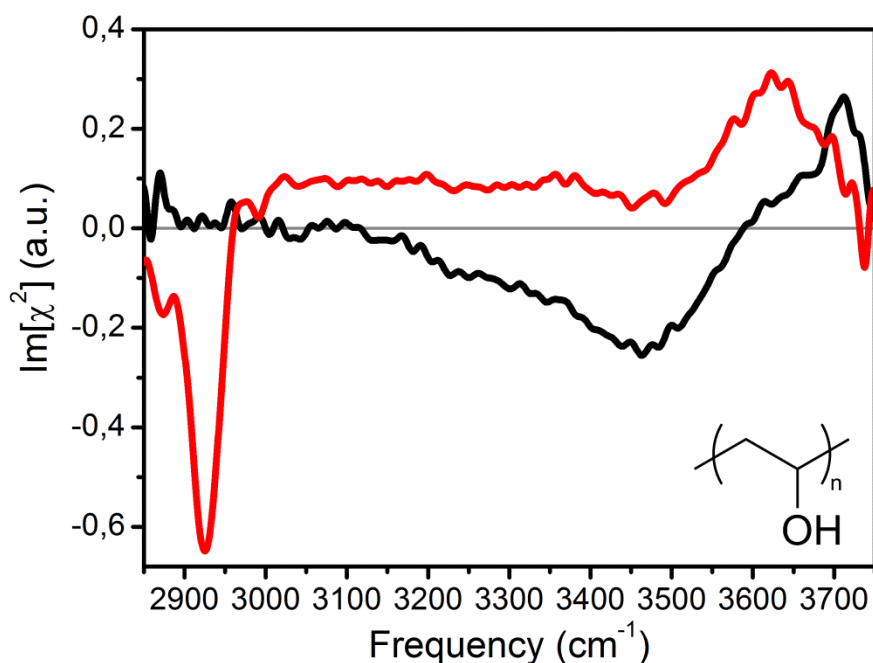


Figure 1: Imaginary $[\chi^{(2)}]$ spectra of pure water (black) and PVA₁₀₀₀₀ (5 wt%, red) at the water-air interface, measured in SSP polarization configuration (s-SFG, s-VIS, p-IR). Inset shows the schematic molecular structure of PVA.

In Figure 1 we present HD-VSFG spectra of pure water and an aqueous 5 wt% PVA₁₀₀₀₀ solution at the water surface, measured with an SSP polarization configuration (s-SFG, s-VIS, p-IR). The presented $\text{Im}[\chi^{(2)}]$ spectrum of pure water is in excellent agreement with results obtained in previous studies^{24,25}. The $\text{Im}[\chi^{(2)}]$ water spectrum shows a broad negative band between 3200 and 3500 cm^{-1} and a narrow positive band at $\sim 3700 \text{ cm}^{-1}$. We assign the broad band to the O-H stretch vibrations of water molecules that form hydrogen bonds to other water molecules. The sharp feature at $\sim 3700 \text{ cm}^{-1}$ is assigned to the O-H stretch vibrations of non-hydrogen bonded O-H-groups that stick out of the surface. The sign of the $\text{Im}[\chi^{(2)}]$ spectrum of the stretch vibration of water is directly related to the orientation of the vibrational transition dipole moment. A positive sign of $\text{Im}[\chi^{(2)}]$ of the O-H stretch vibrations corresponds to a net orientation with the hydrogen atoms pointing towards the air (up), while a negative sign of $\text{Im}[\chi^{(2)}]$ corresponds to hydrogen atoms pointing into the liquid (down).

1
2
3 The $\text{Im}[\chi^{(2)}]$ spectrum of the PVA₁₀₀₀₀ solution strongly differs from that of pure water. In the
4 2800-3000 cm^{-1} region we find narrow peaks that are associated with the C-H vibrations of the
5 polymer backbone. We assign the two negative bands centered at $\sim 2880 \text{ cm}^{-1}$ and $\sim 2930 \text{ cm}^{-1}$ to
6 the stretch vibration of the methine group (ν_{CH}) and to the symmetric stretch of the methylene
7 group ($\nu_{\text{CH}_2,\text{SS}}$), respectively. The positive band at $\sim 2975 \text{ cm}^{-1}$ is assigned to the asymmetric stretch
8 of the methylene group ($\nu_{\text{CH}_2,\text{AS}}$). The negative sign of the $\nu_{\text{CH}_2,\text{SS}}$ and the positive sign of $\nu_{\text{CH}_2,\text{AS}}$,
9 show that the methylene groups have a net orientation with the C-H bonds pointing towards the
10 air phase^{18,24}. The negative sign of the ν_{CH} band suggests that the methine groups are also pointing
11 preferentially towards air. Between 3100 and 3500 cm^{-1} we observe a broad signal that is associated
12 with the O-H stretch vibrations of interfacial water molecules. The positive sign of the signal
13 shows that the interfacial water molecules have a net orientation with the O-H groups pointing
14 away from the bulk. The response that is observed at $\sim 3600 \text{ cm}^{-1}$ is likely due to non-hydrogen-
15 bonded O-H groups sticking out of the surface. However, this signal cannot be due to free OH
16 groups of interfacial water molecules, as those molecules would yield a narrow peak at ~ 3700
17 cm^{-1} , clearly blue shifted from the observed response²⁶. We assign the observed signal at ~ 3600
18 cm^{-1} to the O-H stretch vibrations of non-hydrogen bonded alcohol groups of the PVA chains, in
19 agreement with the results of a previous VSFG study of PVA²⁷. Apparently, PVA is a polymer
20 with a high concentration of hydroxyl groups of which a fraction interacts with the bulk water
21 underneath and a fraction will stick out of the surface.

22
23
24
25
26
27
28
29
30
31
32
33
34
35
36
37 PVA₁₀₀₀₀ has a hydrolysis degree of $\sim 80\%$, which means that $\sim 20\%$ of the acetyl groups have not
38 been hydrolyzed to hydroxyl groups. The ongoing hydrolysis of PVA₁₀₀₀₀ leads to the production
39 of acetic acid and negatively charged acetate ions with a relatively high surface propensity. As a
40 result, the interfacial water molecules have a preferred orientation with their hydrogen atoms
41 pointing towards the surface (away from the bulk), thus explaining the positive sign of the broad
42 spectral response between 3100 and 3500 cm^{-1} . This SFG signal can also be described as a $\chi^{(3)}$
43 effect, where the negative charges at the surface create a static field that orients molecules close
44 to the surface. This orientation results in an asymmetry and thus allows the generation of an SFG
45 signal from the input infrared and visible electric fields. This surface-field induced $\chi^{(3)}$ effect has
46 been studied in detail theoretically^{28,29,30} and has been experimentally observed for surfactants,
47 polyelectrolytes and proteins^{18,24,31,32,33}.

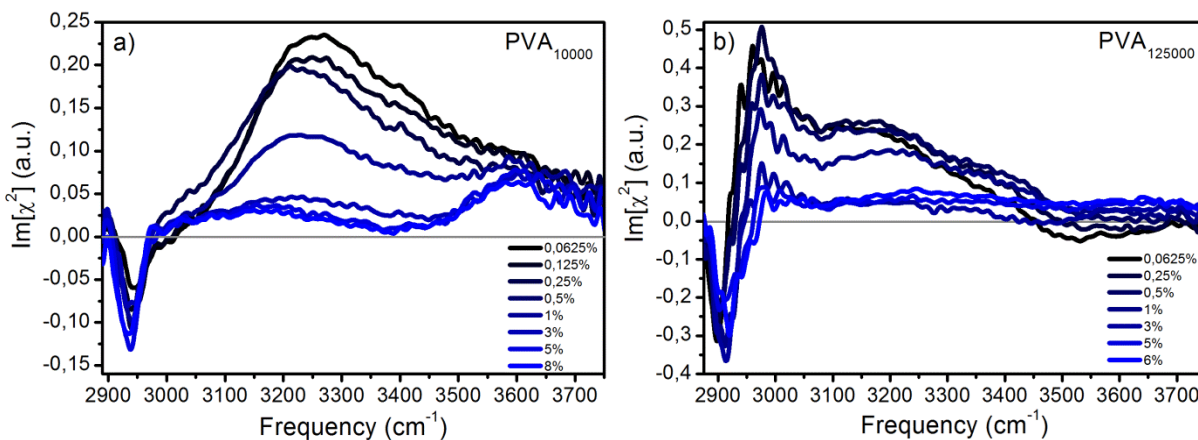


Figure 2: a) Concentration-dependent Imaginary $[\chi^{(2)}]$ spectra of PVA₁₀₀₀₀ and PVA₁₂₅₀₀₀ at the water-air interface, measured in SSP polarization configuration (s-SFG, s-VIS, p-IR). Solution concentrations span from $\sim 0.0625\%$ (black) to $\sim 8\%$ (blue).

In Figure 2a we present $\text{Im}[\chi^{(2)}]$ spectra of aqueous PVA₁₀₀₀₀ solutions with concentrations spanning from $\sim 0.0625\%$ to $\sim 8\%$. At the lowest concentration of $\sim 0.0625\%$ we observe that the broad positive band at $\sim 3200\text{ cm}^{-1}$, attributed to interfacial water molecules, has the highest intensity. With increasing PVA₁₀₀₀₀ concentrations we observe that the intensity of the 3200 cm^{-1} band decreases, confirming the assignment of this band to interfacial water, and at PVA₁₀₀₀₀ concentrations higher than about 1 wt% we find that the intensity is not changing further. A different trend is observed in the C-H region, where the intensity of the signal at $\sim 2970\text{ cm}^{-1}$ first increases and saturates at PVA concentrations higher than about 1 wt%. This last trend is consistent with surface tension measurements that show an initial decrease in γ , and a saturation of this decrease at concentrations $>1\text{ wt}\%$ (Fig. S4)¹².

The strong decrease of the positive $\text{Im}[\chi^{(2)}]$ signal between 3100 and 3500 cm^{-1} with increasing concentration (Figure 2a) can be explained from the reduction of the free water surface. At low concentrations, the surface will not be completely covered with PVA₁₀₀₀₀, and a significant part of the surface consists of water molecules of which the orientation is governed by the surface active acetate ions, yielding to a strong positive signal at $\sim 3200\text{ cm}^{-1}$. When the concentration is increased, the surface will become increasingly covered with a disordered PVA₁₀₀₀₀ polymer film, leading to a decrease of the free water surface and the orienting effect of surface-active acetate

ions. Molecular dynamics (MD) simulations indeed show that at higher concentrations, the PVA polymers occupy both the surface and the subregion of the interface¹⁴.

The $\text{Im}[\chi^{(2)}]$ spectra also show a positive peak centred at 3600 cm^{-1} . This signal can be attributed to the response of the non-hydrogen-bonded hydroxyl groups of PVA_{10000} . The positive sign means that the non-hydrogen-bonded hydroxyl groups have a preferential orientation away from the bulk solution, which is to be expected. We observe negligible spectral changes of this signal upon changing the PVA_{10000} concentration, which suggests that PVA_{10000} does not show large conformational changes when the concentration is increased. The alcohol groups of PVA_{10000} that form hydrogen bonds with water molecules will have a net orientation towards the bulk. The response of these groups likely causes the dip in the signal between 3400 and 3500 cm^{-1} .

In Figure 2b we present the $\text{Im}[\chi^{(2)}]$ spectra of aqueous PVA_{125000} solutions with concentrations ranging from 0.0625% to 6% . PVA_{125000} is much larger than PVA_{10000} and has a higher hydrolysis degree of $\sim 98\%$ ($\sim 2\%$ acetyl groups). The signal in the frequency range 3100 - 3500 cm^{-1} is positive, indicating that the interfacial water molecules have a preferential orientation with their O-H groups away from the bulk, which can again be explained from the ongoing hydrolysis and the production of negatively charged acetate ions that have a relatively high surface propensity. The signal at 3200 cm^{-1} shows the highest intensity at low PVA_{125000} concentrations, and decreases with increasing concentration, but not as strongly as was observed for the smaller PVA_{10000} . Above a concentration of $3\text{ wt}\%$, no further VSFG changes are observed for PVA_{125000} . The increase of the concentration of PVA_{125000} leads to a change of the spectral shape in the CH-region between 2870 and 3000 cm^{-1} . This change in shape is largely due to the fact that the broad and overlapping positive response of the OH vibrations of interfacial water centred at 3200 cm^{-1} decreases. This decrease reduces the observed total positive signal between 2950 and 3000 cm^{-1} while it hardly affects the negative signal between 2870 and 2950 cm^{-1} , thus leading to a change of the overall shape of the spectral response between 2900 and 3000 cm^{-1} .

We find that the VSFG signal between 3500 and 3600 cm^{-1} has a negative sign for low PVA_{125000} concentrations, which is quite different from the observations for the PVA_{10000} solutions. This negative signal corresponds to weakly and non-hydrogen bonded hydroxyl groups of the PVA chains. This finding suggests that PVA_{125000} polymers acquire a special folded conformation in which the alcohol groups have a net orientation towards the aqueous solution. Such a preferential

orientation towards the bulk agrees with the result of a molecular simulation study on 100% hydrolyzed PVA¹⁴. We observe that the 3500-3600 cm^{-1} signal becomes positive at high concentrations, which indicates that the polymer undergoes a significant conformational change in the surface region at high concentrations.

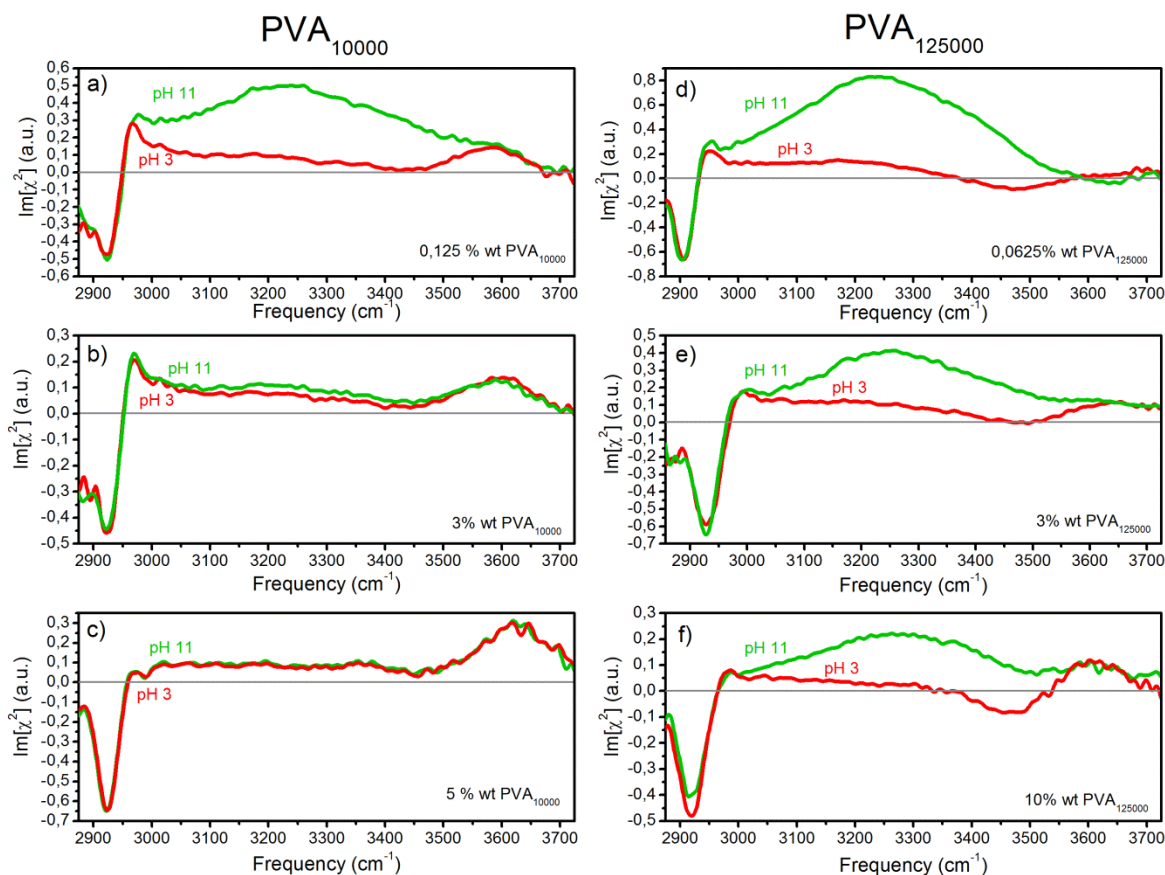


Figure 3: a) Concentration-dependent Imaginary $[\chi^{(2)}]$ spectra of PVA₁₂₅₀₀₀ at the solution-air interface. Solution concentrations span from $\sim 0.0625\%$ (black) to $\sim 6\%$ (blue). b) pH-dependent Imaginary $[\chi^{(2)}]$ spectra of PVA₁₂₅₀₀₀ at low concentrations. c) pH-dependent Imaginary $[\chi^{(2)}]$ spectra of PVA₁₂₅₀₀₀ at high concentrations.

In Figure 3a we present PVA₁₀₀₀₀ spectra at a low concentration for two different pH values. Lowering the pH value causes the signal at $\sim 3200 \text{ cm}^{-1}$ to decrease significantly in intensity due to the neutralization of the negative acetate ions. In Figures 3b and 3c we present pH-dependent

1
2
3 PVA₁₀₀₀₀ spectra at high concentrations. In contrast to Figure 3a, we find that the solution pH has
4 a negligible effect on the amplitude of the interfacial water signal centred at $\sim 3200\text{ cm}^{-1}$. The signal
5 of the hydrogen-bonded water molecules remains low for an alkaline solution with pH=11. We
6 also observe no changes for the PVA specific signals at $\sim 2970\text{ cm}^{-1}$ and $\sim 3600\text{ cm}^{-1}$.
7
8
9

10
11 When we increase the PVA₁₀₀₀₀ concentration, the surface gets completely covered with a
12 disordered polymer layer and the interfacial water signal becomes very small. In this limit, the pH
13 has little effect on the magnitude of the signal, because there is no water surface at which
14 negatively charged acetate ions can accumulate. Hence, also at high pH there will be no net
15 orienting effect on the interfacial water molecules, and thus the signal remains low.
16
17
18
19

20
21 In Figure 3d we show $\text{Im}[\chi^{(2)}]$ spectra of a low concentration PVA₁₂₅₀₀₀ solution at two different
22 pH values. When the pH is decreased we observe a strong decrease in the intensity of the broad
23 signal centred at 3200 cm^{-1} . We explain this signal decrease again from the neutralization of the
24 acetate ions. In Figures 3e and 3f, we present $\text{Im}[\chi^{(2)}]$ spectra of a high concentration PVA₁₂₅₀₀₀
25 solution at two different pH values. At high pH we observe a significantly stronger $\text{Im}[\chi^{(2)}]$ signal
26 near 3200 cm^{-1} than at low pH. This observation is quite different from the results obtained for the
27 smaller PVA₁₀₀₀₀ polymers for which very little dependence on pH was observed at high polymer
28 concentrations. This finding shows that a concentrated PVA₁₂₅₀₀₀ polymer solution contains a
29 relatively high density of interfacial water molecules of which the orientation depends on the pH,
30 which indicates that the surface contains regions where water is in direct contact with air and where
31 acetate ions can accumulate. Hence, this finding indicates that the surface of a highly concentrated
32 solution of PVA₁₂₅₀₀₀ possesses open spaces.
33
34
35
36
37
38
39
40
41

42 Recently, Rošić et al. reported that for PVA₁₂₅₀₀₀ concentrations above 5%, the surface tension of
43 the PVA solution rises with increasing polymer concentration and reaches the value of pure water
44 at concentrations higher than $\sim 10\%^4$. We observe a similar surface tension anomaly (Fig. S5).
45 Interestingly, we can still detect VSFG signals of the C-H vibrations of PVA₁₂₅₀₀₀ even at a high
46 concentration of 10% (Figure 3f), which shows that a significant amount of PVA remains present
47 at the surface, despite the surface tension values becoming similar to water. The combination of
48 the surface tension data with the VSFG data indicates that at high concentrations of PVA₁₂₅₀₀₀, the
49 polymers in the surface region aggregate to form pores, thus leading to a direct contact between
50 surface water and air. The formation of such an extremely inhomogeneous interfacial solution
51
52
53
54
55
56
57
58
59
60

1
2
3 configuration explains why both the PVA polymer and the interfacial water signals remain to be
4 observed, and why the surface tension shows an anomalous increase with concentration in the
5 regime of high PVA₁₂₅₀₀₀ concentrations. In addition, a conformational transition of the PVA₁₂₅₀₀₀
6 polymer chains from a more stretched arrangement at low concentrations to a more compact,
7 aggregated conformation at higher concentrations can also explain the change in sign of the 3500-
8 3600 cm⁻¹ signal when the concentration is increased (Figure 2b).
9
10
11
12
13

14 **Conclusions**

15
16
17 We studied the properties of the surface of aqueous solutions of polyvinyl alcohol polymers with
18 average molecular weights of 10000 g/mol and 125000 g/mol using heterodyne-detected
19 vibrational sum-frequency generation spectroscopy. This technique allows us to determine Im[$\chi^{(2)}$]
20 over a wide frequency range, from which we can derive information on the orientation of the
21 interfacial water molecules and the orientation and conformation of the PVA molecules.
22
23
24
25

26
27 The Im[$\chi^{(2)}$] spectrum of the interfacial water molecules has a positive sign for both PVA₁₀₀₀₀ and
28 PVA₁₂₅₀₀₀ at all studied concentrations, which implies that the interfacial water molecules have a
29 preferred orientation with their O-H groups pointing away from the bulk. This observation can be
30 explained from the presence of negatively charged acetate ions that are produced by the ongoing
31 hydrolysis of the acetyl impurities on the PVA polymer chains. We observe Im[$\chi^{(2)}$] to be positive
32 for the response of the non-hydrogen-bonded hydroxyl groups of PVA₁₀₀₀₀, indicating that these
33 groups are sticking out of the surface.
34
35
36
37
38

39
40 For solutions containing a low concentration of PVA₁₀₀₀₀ or PVA₁₂₅₀₀₀ the interfacial water signal
41 strongly decreases with decreasing pH because of the neutralization of the acetate ions. For highly
42 concentrated solutions of PVA₁₀₀₀₀ polymers the signal becomes very small, irrespective of the
43 pH, indicating that the surface is completely covered with a disordered PVA₁₀₀₀₀ polymer film.
44 For highly concentrated solutions of PVA₁₂₅₀₀₀ polymers, the interfacial water signal remains pH
45 dependent, getting large at high pH values, which indicates that these concentrated polymer
46 solutions still contain a relatively high density of interfacial water molecules. This relatively high
47 density of interfacial water is consistent with the anomaly in the surface tension that has been
48 observed for large molecular weight PVA polymer solutions. For these solutions, the surface
49 tension first decreases, as is commonly observed for surfactant molecules, but beyond a certain
50
51
52
53
54
55
56
57
58
59
60

1
2
3 concentration (~3%) the surface tension re-rises. Combining this finding with the present $\text{Im}[\chi^{(2)}]$
4 spectra we propose that large molecular weight PVA polymer solutions form aggregated pores in
5 the interfacial region, thus allowing for a high density of interfacial water.
6
7
8
9
10
11
12
13
14
15
16
17
18
19
20
21
22
23
24
25
26
27
28
29
30
31
32
33
34
35
36
37
38
39
40
41
42
43
44
45
46
47
48
49
50
51
52
53
54
55
56
57
58
59
60

Supporting Information:

Figure S1: Schematic representation of ester hydrolysis on PVA polymer chains; Figure S2: Surface Tension measurements of PVA₁₀₀₀₀; Figure S3: Variation of pH values of PVA with concentration Figure S4: Surface Tension measurements of PVA₁₂₅₀₀₀.

Acknowledgements:

This work is part of the research program of the Netherlands Organization for Scientific Research (NWO) and was performed at the research institute AMOLF. This project has received funding from the European Research Council (ERC) under the European Union's Horizon 2020 research and innovation program (grant agreement No 694386).

References:

1. Andreassen, S. Ø.; Chong, S.-F.; Wohl, B. M.; Goldie, K. N.; Zelikin, A. N., Poly(vinyl alcohol) Physical Hydrogel Nanoparticles, Not Polymer Solutions, Exert Inhibition of Nitric Oxide Synthesis in Cultured Macrophages. *Biomacromolecules* **2013**, *14* (5), 1687-1695.
2. Tummala, G. K.; Joffre, T.; Rojas, R.; Persson, C.; Mihranyan, A., Strain-Induced Stiffening of Nanocellulose-Reinforced Poly(vinyl alcohol) Hydrogels Mimicking Collagenous Soft Tissues. *Soft Matter* **2017**, *13*, 3936-3945.
3. Bannerman, D.; Li, X.; Wan, W., A 'degradable' poly(vinyl alcohol) iron oxide nanoparticle hydrogel. *Acta Biomater* **2017**, *58*, 376-385.
4. Rošič, R.; Pelipenko, J.; Kristl, J.; Kocbek, P.; Bešter-Rogač, M.; Baumgartner, S., Physical Characteristics of Poly (vinyl alcohol) Solutions in Relation to Electrospun Nanofiber Formation. *European Polymer Journal* **2013**, *49* (2), 290-298.
5. López-Rubio, A.; Sanchez, E.; Sanz, Y.; Lagaron, J. M., Encapsulation of Living Bifidobacteria in Ultrathin PVOH Electrospun Fibers. *Biomacromolecules* **2009**, *10* (10), 2823-2829.
6. Choi, J.-H.; Jegal, J.; Kim, W.-N.; Choi, H.-S., Incorporation of Multiwalled Carbon Nanotubes into Poly(vinyl alcohol) Membranes for Use in the Pervaporation of Water/ethanol Mixtures. *Journal of Applied Polymer Science* **2009**, *111* (5), 2186-2193.
7. Ahn, S.-M.; Ha, J.-W.; Kim, J.-H.; Lee, Y.-T.; Lee, S.-B., Pervaporation of fluoroethanol/water and methacrylic acid/water mixtures through PVA composite membranes. *Journal of Membrane Science* **2005**, *247* (1-2), 51-57.
8. Fejerskov, B.; Smith, A. A. A.; Jensen, B. E. B.; Hussmann, T.; Zelikin, A. N., Bioresorbable Surface-Adhered Enzymatic Microreactors Based on Physical Hydrogels of Poly(vinyl alcohol). *Langmuir* **2013**, *29* (1), 344-354.
9. Congdon, T.; Notman, R.; Gibson, M. I., Antifreeze (Glyco)protein Mimetic Behavior of Poly(vinyl alcohol): Detailed Structure Ice Recrystallization Inhibition Activity Study. *Biomacromolecules* **2013**, *14* (5), 1578-1586.
10. Budke, C.; Koop, T., Ice Recrystallization Inhibition and Molecular Recognition of Ice Faces by Poly(vinyl alcohol). *ChemPhysChem* **2006**, *7* (12), 2601-2606.
11. Inada, T.; Lu, S.-S., Thermal Hysteresis Caused by Non-Equilibrium Antifreeze Activity of Poly(vinyl alcohol). *Chemical Physics Letters* **2004**, *394* (4-6), 361-365.
12. Bhattacharya, A.; Ray, P., Studies on Surface Tension of Poly(vinyl alcohol): Effect of Concentration, Temperature, and Addition of Chaotropic Agents. *Journal of Applied Polymer Science* **2004**, *93* (1), 122-130.
13. Matsuzawa, S.; Yamaura, K.; Yoshimoto, N.; Horkawa, I.; Kuroiwa, M., Adsorption of Stereoregular Poly(vinyl alcohols) at Air-Water Interface. *Colloid & Polymer Sci* **1980**, *258* (2), 131-135.
14. Tesei, G.; Paradossi, G.; Chiessi, E., Influence of Surface Concentration on Poly(vinyl alcohol) Behavior at the Water-Vacuum Interface: A Molecular Dynamics Simulation Study. *The Journal of Physical Chemistry B* **2014**, *118* (24), 6946-6955.
15. De Feijter, J. A.; Benjamins, J., Adsorption Behavior of PVA at the Air-Water Interface i. Applicability of the Gibbs Adsorption Equation. *Journal of Colloid and Interface Science* **1981**, *81* (1), 91-107.
16. Cengiz, F.; Dao, T. A.; Jirsak, O., Influence of Solution Properties on the Roller Electrospinning of Poly(vinyl alcohol). *Polymer Engineering & Science* **2010**, *50* (5), 936-943.
17. Shen, Y. R., Surface Properties Probed by Second-Harmonic and Sum-Frequency Generation. *Nature* **1989**, *337* (6207), 519-525.

- 1
2
3 18. Balzerowski, P.; Meister, K.; Versluis, J.; Bakker, H. J., Heterodyne-Detected Sum Frequency
4 Generation Spectroscopy of Polyacrylic Acid at the Air/Water-Interface. *Physical Chemistry Chemical*
5 *Physics* **2016**, *18* (4), 2481-2487.
- 6 19. Hu, D.; Yang, Z.; Chou, K. C., Interactions of Polyelectrolytes with Water and Ions at Air/Water
7 Interfaces Studied by Phase-Sensitive Sum Frequency Generation Vibrational Spectroscopy. *The Journal*
8 *of Physical Chemistry C* **2013**, *117* (30), 15698-15703.
- 9 20. Lu, X.; Zhang, C.; Ulrich, N.; Xiao, M.; Ma, Y.-H.; Chen, Z., Studying Polymer Surfaces and Interfaces
10 with Sum Frequency Generation Vibrational Spectroscopy. *Analytical Chemistry* **2017**, *89* (1), 466-489.
- 11 21. Shen, Y. R., Phase-Sensitive Sum-Frequency Spectroscopy. *Annu Rev Phys Chem* **2013**, *64*, 129-
12 150.
- 13 22. Hallensleben, M. L., Polyvinyl Compounds, Others. In *Ullmann's Encyclopedia of Industrial*
14 *Chemistry*, Wiley-VCH Verlag GmbH & Co. KGaA: 2000.
- 15 23. Minofar, B.; Vácha, R.; Wahab, A.; Mahiuddin, S.; Kunz, W.; Jungwirth, P., Propensity for the
16 Air/Water Interface and Ion Pairing in Magnesium Acetate vs Magnesium Nitrate Solutions: Molecular
17 Dynamics Simulations and Surface Tension Measurements. *The Journal of Physical Chemistry B* **2006**, *110*
18 (32), 15939-15944.
- 19 24. Nihonyanagi, S.; Yamaguchi, S.; Tahara, T., Direct Evidence for Orientational Flip-Flop of Water
20 Molecules at Charged Interfaces: A Heterodyne-Detected Vibrational Sum Frequency Generation Study.
21 *The Journal of Chemical Physics* **2009**, *130* (20), 204704.
- 22 25. Chen, X.; Hua, W.; Huang, Z.; Allen, H. C., Interfacial Water Structure Associated with Phospholipid
23 Membranes Studied by Phase-Sensitive Vibrational Sum Frequency Generation Spectroscopy. *Journal of*
24 *the American Chemical Society* **2010**, *132* (32), 11336-11342.
- 25 26. Du, Q.; Superfine, R.; Freysz E.; Shen Y. R., Vibrational spectroscopy of water at the vapor/water
26 interface. *Physical Review Letters* **1993**, *70*, 2313-2316.
- 27 27. Zuo, B.; Hu, Y.; Lu, X.; Zhang, S.; Fan, H.; Wang, X., Surface Properties of Poly(vinyl alcohol) Films
28 Dominated by Spontaneous Adsorption of Ethanol and Governed by Hydrogen Bonding. *The Journal of*
29 *Physical Chemistry C* **2013**, *117* (7), 3396-3406.
- 30 28. Ohono, P. E.; Wang, H.-F.; Geiger, F. M., Second-order spectral lineshapes from charged
31 interfaces. *Nature Communications* **2017**, *8*, 1032.
- 32 29. Ohno, P. E.; Wang, H.-F.; Paesani, F.; Skinner, J. L.; Geiger, F. M., Second-Order Vibrational
33 Lineshapes from the Air/Water Interface. *Journal of Physical Chemistry* **2018**, *122*, 4457-4464.
- 34 30. Reddy, S. K.; Thiriaux, R.; Wellen Rudd, B. A.; Lin, L.; Adel, T.; Joutsuka, T.;
35 Geiger, F. M.; Allen, H. C.; Morita, A.; Paesani, F.; Bulk Contributions Modulate the SFG Spectra of Water
36 on Model Sea-Spray Aerosols. *Chem* **2018**, *4* (7), 1629-1644.
- 37 31. Wen, Y.-C.; Zha, S.; Yang, S.; Guo, P.; Shi, G.; Fang, H.; Shen, Y. R.; Tian, C., Unveiling Microscopic
38 Structures of Charged Water Interfaces by Surface-Specific Vibrational Spectroscopy. *Physical Review*
39 *Letters* **2016**, *116*, 016101.
- 40 32. Strazdaite, S.; Meister, K.; Bakker, H. J., Orientation of Polar Molecules near Charged Protein
41 Interfaces. *Physical Chemistry Chemical Physics* **2016**, *18* (10), 7414-7418.
- 42 33. Meister, K.; Paananen, A.; Bakker, H. J., Identification of the Response of Protein N-H Vibrations
43 in Vibrational Sum-Frequency Generation Spectroscopy of Aqueous Protein Films. *Physical Chemistry*
44 *Chemical Physics* **2017**, *19* (17), 10804-10807.
- 45
46
47
48
49
50
51
52
53
54
55
56
57
58
59
60

TOC Graphic

